Polymer Bulletin (2023) 80:5333–5352
https://doi.org/10.1007/s00289-022-04270-7

ORIGINAL PAPER

# Green synthesis of chitosan-silver nanocomposite reinforced with curcumin nanoparticles: characterization and antibacterial effect

**Zahra Rajabloo[1] · Elahe Mobarak Qamsari[1] · Rouha Kasra Kermanshahi[1] · Faezeh Farzaneh[2]**

Received: 24 January 2022 / Revised: 27 March 2022 / Accepted: 28 April 2022 /
Published online: 27 June 2022


## Abstract

There has been significant interest to finding new and effective bactericidal materials due to increasing antibiotic resistance. Herein, this work reports on the design of a chitosan nanocomposite (NC) with two nanoparticle (NP) components, silver (Ag) and curcumin nanoparticles (Cur-NPs) with enhanced antibacterial activity. Chitosan-silver curcumin NC (Chi-Ag Cur NC) was prepared by adding water-soluble Cur-NPs to Chi-Ag NC solution. In order to produce Chi-Ag NC in a green manner, silver nanoparticles (Ag-NPs) were synthesized through photochemical reduction by using chitosan as the stabilizing agent and acetic acid as the reducing agent. The characteristics of Chi-Ag Cur NC were investigated through UV–Vis spectroscopy, FTIR, XRD, EDX, SEM, and DLS analysis. Chi-Ag Cur NC's antibacterial activity was further tested against certain clinically isolated strains of burn wound infection with significant antibiotic resistance as well as some standard bacterial strains. An increase in antimicrobial/antibiofilm activity of Chi-Ag Cur NC was observed with lower MIC and MBIC. In addition, no cytotoxicity of freshly produced NC was seen in NHDF cells. These results clearly revealed the synergy of Ag-NPs and Cur-NPs in novel antibacterial NC film which can be applicable as a promising antibacterial coating to prevent infection and promote burn wound healing.

✉ Rouha Kasra Kermanshahi
rkasra@yahoo.com

Zahra Rajabloo
rajablooz@yahoo.com

Elahe Mobarak Qamsari
emobarak110@gmail.com

Faezeh Farzaneh
Faezehfarzaneh@yahoo.com

[1] Department of Microbiology, Faculty of Biosciences, Alzahra University, Tehran, Iran

[2] Department of Chemistry, Faculty of Physics & Chemistry, Alzahra University, Tehran, Iran

**Keywords** Chitosan · Silver · Curcumin · Nanocomposite · Wound infection

## Introduction

Burn wound bacteria generate a slew of issues in individuals suffering from acute burn wound infections. Many of these bacteria are resistant to most antibiotics, making treatment more difficult in these patients [1]. Antibiotic resistance has spread throughout the world as antibiotic use has increased [2]. The quest for finding novel and effective bactericidal materials is critical for combating drug resistance, and nanoparticles (NPs) have emerged as a viable method to addressing this issue. The large surface area-to-volume ratio of NPs has made them a unique delivery and antimicrobial agents in many respect [3–5]. NP-based therapies have an expansive range of applications in wound healing. Furthermore, the creation of innovative bio-composite materials impregnated with metal NPs might be a more effective wound healing therapy technique with efficient antibacterial activity [6]. The synthesis of nanocomposite (NC) materials based on chitosan and silver NPs (Ag-NPs) is currently of great interest in biomedical and pharmaceutical fields because of their strong antimicrobial features [7–9]. Chitosan, a linear cationic polysaccharide made up of randomly repeated units of β-(1, 4) coupled N-acetyl glucosamine, is produced by partial N-deacetylation of chitin [10, 11]. Amino acids groups with positive charge in the chitosan structure interact with negative bacterial cell wall components; hence, inducing cell wall and membrane disruption [12]. Furthermore, it is attested by many researchers that this significant anti-bactericidal impact is due to chitosan propensity for penetrating into the microbial membranes and inhibiting DNA replication [6]. Ag-NPs play a significant role in the field of bio-medicine due to its unique physiochemical properties such as antibacterial, antifungal, anti-inflammatory properties [13]. When Ag-NPs are combined with chitosan, it has the potential to accelerate the wound healing process with excellent antimicrobial activities. Antimicrobial activity is mediated by attaching to the negatively charged bacterial cell wall, resulting in cell envelope instability and altered permeability [14]. Curcumin is a nutraceutical agent with several pharmacological properties, and it has potent therapeutic activity in wound healing applications [15]. Curcumin is a hydrophobic polyphenolic chemical derived from turmeric, the powdered rhizome of *Curcuma longa* with potent biological properties [16]. However, its biomedical application is limited by its low solubility in water. To address this issue, several researchers have reported the nanoformulation of curcumin utilizing natural polymers such as chitosan and alginate [17]. Furthermore, the combination of curcumin with metal-based NPs (such as silver and titanium) result in synergistic antibacterial effects [15].

The ability of nanocurcumin along with Ag-NPs to act as nano-reinforcements within the chitosan matrix and their antibacterial properties have been less studied. Given the improved microbiological inhibition of chitosan-silver NC (Chi-Ag NC) compared solely to chitosan and Ag-NPs, combining NC with curcumin NP (Cur-NP) may be a viable approach in the battle against several types of bacteria, particularly in the treatment of wound infections. As a result, the goal of this research is to create a chitosan NC with two NP components, silver and Cur-NP,

to improve therapeutic properties. Chitosan-silver-curcumin NC (Chi-Ag Cur NC) was produced using a green and environmentally friendly approach. We also studied the physicochemical properties and cytotoxicity of Chi-Ag Cur NC. Furthermore, the antibacterial and antibiofilm properties of Chi-Ag NC and Chi-Ag-Cur NC were evaluated against clinical bacterial isolates related with wound infections, as well as some standard bacterial strains. It was recognized to be extremely effective in killing both planktonic and biofilm-forming bacteria. The prepared Chi-Ag-Cur NC film can be a new type of biopolymer-based wound dressing for burn wound infection treatments.

## Material and methods

### Materials

The chitosan high molecular weight Mw 310,000–375,000 Da, > 75% deacetylated, silver nitrate, and curcumin were obtained from Sigma-Aldrich, USA. Other chemicals utilized in this investigation were acetic acid glacial, glycerol, sodium bicarbonate, nutrient agar, nutrient broth, Moller Hinton agar (MHA), and Tryptic soy broth (TSB), which were obtained from Merck in Germany without further purification. Iranian Research Organization for Science and Technology provided the standard bacterial strains and cell line (IROST).

### Preparation of Chi-Ag-Cur NC

The synthetic procedure followed for the preparation of Chi-Ag-Cur NC consists of the following three steps, as revealed, schematically, in Scheme 1.

(i) The preparation of Chi-Ag NC:
Chitosan solution (1% w/v) was made in an electric oven at 70 °C by dissolving chitosan in acetic acid solution (1% v/v) for at least 1 h until a clear solution produced. The flask holding the chitosan solution was placed on the magnetic stirrer, and 100 mg of silver nitrate was progressively added to it and then was placed under sunlight. The production of Ag-NPs solution is indicated by a shift in hue from cream to dark brown. The flask was then put in a 100 W ultrasonic bath for 10 min to avoid the agglomeration of Ag-NPs [18].

(ii) The preparation of Cur-NPs:
To create a clear solution, 100 ml of sodium bicarbonate buffer 4 M was made and put on a magnetic stirrer at 120 °C. The temperature was subsequently lowered to 100 °C, and a dropwise addition of 0.1 M curcumin solution in ethanol (10 ml) into the boiling buffer was performed using a sampler. For 8 h, the solution was agitated on a magnetic stirrer at 100 °C until the yellow hue turned to red. The formation of sodium curcumin salt is indicated by the change in solution color. The solution was then centrifuged

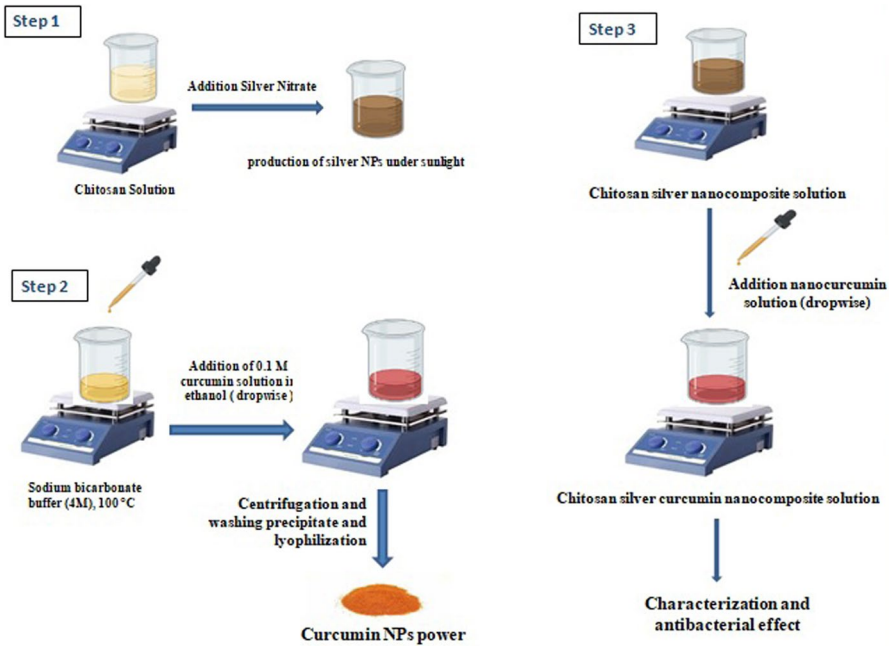


**Scheme 1** Synthesis procedure followed for the preparation of Chi-Ag-Cur NC

(11,000 rpm, 25 °C, 30 min). The precipitate that formed was rinsed with 15 mL of distilled water. The final precipitate was collected and dried in a 70 °C oven. After dissolving the dried curcumin salt in 100 mL of distilled water, it was put in an ultrasonic bath for 1 h. The entire contents were then put into a plastic container with multiple holes in the top and frozen for 24 h at – 80 °C. Cur-NPs were produced during an 18-h lyophilization process. The Cur-NPs powder was then put into a disposable plate and sterilized under UV light for 1 h before being poured into a sterile dark container and kept in a refrigerator at 4 °C [19].

(iii) The formation of Chi-Ag-Cur NC:

Chi-Ag-Cur NC solution was made by dissolving 0.1 gr of freeze-dried Cur-NPs powder in 20 ml of distilled water and adjusting the pH to 7. Then, using a magnetic stirrer at 70 °C for 15 min, 20 ml of Cur-NPs powder solution was gently added to 50 ml of Chi-Ag NC solution. To produce the Chi-Ag-Cur NC film, all of the flask contents were poured onto the bottom of a square-shaped Pyrex glass container and dried in a dry-heat oven for 10 min. After that, 50 ml of 1 molar NaOH was produced and put onto the dried film in the Pyrex container before being placed in the dry-heat oven for a second time. After removing the film from the container bottom, it was rinsed three times with distilled water and sterilized in a Petri dish for 20 min under UV light.

### Characterization of prepared NCs

Shidmadzu UV–visible spectrophotometer (UV-1800-Tokyo, Japan) was used to measure the UV–visible spectral range from 350 to 800 nm. All sample solutions were diluted one–ten. Using a Dynamic Light Scattering (DLS) instrument, the particle size and polydispersity index (PDI) of produced NCs were assessed. VEGA TESCAN-LMU Scanning Electron Microscopy was used to examine the surface morphologies of the NC films (SEM). Small pieces of prepared NC film were cut and put on a platinum substrate. Surface coating with gold was used to increase the electrical conductivity of the samples, which was then examined using SEM. The elemental analysis was carried out with the use of a SEM attachment named Energy Dispersive X-ray (EDX). The Fourier Transform infrared (FTIR) spectra were also collected using a Series 100 Perkin Elmer 1650 FTIR spectrophotometer (Waltham, MA, USA) in the 400–4000 $cm^{-1}$ range. KBr powder was used to make pellets of freeze-dried samples (0.1 g). The structures of the produced NCs were investigated using Philips X'pert Pro Panalytical PW3040MPD X-ray diffraction (XRD).

### Antibacterial activity

The produced NCs were evaluated in-vitro against four isolated strains from burn wound infection patients. Clinical strains with the highest antibiotic resistance were chosen from a pool of 120 clinically isolates. These isolates were characterized and identified based on their morphological, cultural, and biochemical features. The results showed that the K5, Pst14, E18, and S3 isolates are closely related to *Klebsiella pneumonia* (*K. pneumonia)*, *Pseudomonas aeruginosa* (*P. aeruginosa)*, *Escherichia coli* (*E. coli)*, and *Staphylococcus aureus* (*S. aureus)*, respectively. In addition, a number of standard strains including *K. pneumoniae* (ATCC 7000603), *P. aeruginosa* (ATCC 27853), *E. coli* (ATCC 25922), and *S. aureus* ATCC (25923) were evaluated.

#### Kirby-bauer disk diffusion assay

The antibacterial performance of two Chi-Ag NC and Chi-Ag-Cur NC against clinical and reference isolates was determined using the disc diffusion test (Kirby-Bauer). Each strain was swabbed on a solid MHA after an overnight culture. Chi-Ag NC and Chi-Ag-Cur NC films were cut into 5-mm-diameter circles. After UV sterilization, the NCs films were put over the plates and incubated for 24 h at 37° C. The zone of inhibition's diameter was measured in millimeters. Agar well diffusion method is used to evaluate the antimicrobial activity of Cur-NPs.

#### Minimum inhibitory concentration (MIC)

For the MIC test, Müller–Hinton Broth (MHB) and TSB media were employed. Each strain was transferred to a 5-mL TSB tube and cultured overnight at 37° C. The

bacterial cultures were then diluted, and the tube's turbidity was set to $1 \times 10^6$ (CFU/mL). The MIC was determined using the dilution method in 96-well plate microtiter according to the CLSI M07-A9 standard [20]. All 12 wells received 100 µl of sterile MHB. The first well, which contains the most antimicrobial agent, contains 1500 and 625 µg/ml of Chi-Ag NC and Chi-Ag-Cur NC solution, respectively. The starting concentrations of Chi-Ag NC and Chi-Ag-Cur NC solution in standard strains were 375 and 312.5 µg/ml, respectively. Sum 100 µl of NC and 100 µl of bacterial suspension were added to the negative control well and the positive control well, respectively. Finally, the data were recorded using an ELISA reader at 630 nm. The MIC was determined as the lowest antibacterial concentration that completely inhibited visible growth of the test strains within a specified time period.

### Minimum biofilm inhibitory concentration (MBIC) and minimum biofilm eradication concentration (MBEC)

MBIC and MBEC tests were performed by broth microdilution method in adherent 96-well microtiter plates [21]. The optical density (OD) of adherent bacteria was measured at 550 nm using an ELISA plate reader. The Chi-Ag NC and Chi-Ag-Cur NC stock solutions were prepared to a concentration of 12,000 µg/ml and 1000 µg/ml (MBIC tests) and 6000 µg/ml and 5000 µg/ml, respectively (MBEC tests). TSB medium supplemented with 0.2% glucose (TSG) was used for MBIC and MBEC experiments. Each strain was transferred to 5 mL of TSG and cultivated overnight at 37 ˚C. The bacterial cultures were then diluted and the turbidity of the tube was set to $1 \times 10^6$ (CFU/mL). An aliquot of 100 µl of sterile TSG was added to all 12 wells. The first well contained the highest concentration of antimicrobial agent as 3000 and 2500 µg/ml of Chi-Ag NC and Chi-Ag-Cur NC, respectively. Negative control wells were only filled with 100 µl of NC. Positive control wells were only filled with 100 µl of bacterial suspension. The microtiter plate was then incubated at 37 °C for 24 h. Media was removed from all wells after the respective incubation times. The formed biofilm was rinsed with physiological serum. At this point, spectrophotometric evaluation of the biofilm development was not feasible since its optical density was below the detection limit of the plate reader. After rinsing, 100 µl of the sterile TSG was added to the wells. Each plate was incubated again for 24 h at 37˚˚C to allow biofilm development. The plates were then stained with 0.2% solution of crystal violet (200 µl each well) for 15 min. Then, crystal violet solution was removed and wells were rinsed three times with sterile physiological serum. During the rinsing care was exercised as to avoid any possible biofilm disturbance. The plate was dried at room temperature. Next, 200 µl of 30% glacial acetic acid was added to each well. After 15 min, the absorbance was read at 550 nm using an ELISA plate reader [22]. The percentage of biofilm inhibition in each well was calculated as:

$$\text{Biofilm formation } (\%) = \frac{(A) - (B)}{(C) - (B)} \times 100$$

A: Optical absorption of the tested well.
B: Optical absorption of the negative well.

C: Optical absorption of the positive well.

Biofilm removal rate in each of the tested wells was calculated using the following formula:

$$\text{Biobilm inhibiton } (\%) = 100 - (\text{Biofilm formation})$$

### Cytotoxicity test

In a 96-well plate, Normal Human Dermal Fibroblasts (NHDF) cells were seeded at a density of $10^5$ cells per well in Dulbecco's Modified Eagle's medium (DMEM) with 10% Fetal bovine serum (FBS) and then cultured at 37 °C for 24 h with 5% CO2. The prepared plate was rinsed twice with phosphate-buffered saline (PBS). Then, 100 µl from different concentrations of Chi-Ag NC and Chi-Ag-Cur NC were added to each well (1–1000 µg/ml).Wells treated with 1% Triton X100 were used as the negative control and untreated wells were selected as the positive control. The cells were further incubated for 24 h. Then cells were rinsed twice with PBS. Thereafter, 225 µl of fresh growth medium and 25 µl of 0.5 mg/ml 3-(4,5-dimethylthiazol-2-yl)-2,5-diphenyltetrazolium bromide (MTT) were added to each well and the cells were incubated for four hours. After incubation, the unreduced MTT and the medium were removed and 250 µl of DMSO was added to each well as to dissolve the MTT formazan crystals. Finally, the absorbance of formazan product was read at 540 nm using an ELISA plate reader [23]. The following formula was used to compute the survival percentage in comparison with the control cells (100% survival):

$$\text{Suvival percentage} = \frac{\text{A}}{\text{B}} \times 100$$

A: Each NC concentration's absorption.

B: Positive control absorption.

## Results and discussion

### Preparation of NCs

Chemical reduction, electrochemical, irradiation, and thermal decomposition are some of the techniques used to produce NPs. Toxic, hazardous substances are employed in the majority of chemical techniques used to synthesize NPs. Green synthesis methods have been developed to manufacture NPs to address the disadvantages of hazardous substances [24]. The production of Ag-NPs utilizing organic acids (acetic acid or ascorbic acid) and UV (or visible light) irradiation might be described as the green approaches [25]. Ag-NPs were synthesized using photochemical reduction utilizing chitosan as the stabilizing agent and acetic acid (organic acid) as the reducing agent to create Chi-Ag NC in an environmentally friendly method. Polymers possessing amino groups, such as chitosan, can diminish metal ions. In line with our results, [26] also synthesized Chi-Ag NC by acetic acid as the reducing agent and chitosan as the

stabilizing agent [26]. Chi-Ag NC was created in this work by utilizing chitosan with deacetylation of > 75%, which decreased the photochemical reduction time from 1 h to 5 min. Thomas et al. (2009) managed to generate Chi-Ag NC films in a green manner utilizing a photochemical reduction process, but they had to first deacetylate chitin to produce chitosan, thus when exposed to sunlight, one hour was required for the color change and creation of Ag-NPs [27]. As mentioned, in this study the synthesis of Chi-Ag NC was carried out in a green manner and without any chemical reductive agents through photochemical reduction and using a chitosan acidic solution. Vimala et al. (2011) used the photochemical reduction method to produce a Chi-Ag NC film by using polyvinyl alcohol and glutaraldehyde. The newly-formed NC cannot be classified as a green product due to the presence of polyvinyl alcohol and glutaraldehyde [28].

In this study, Cur-NPs were produced using sodium bicarbonate buffer. Furthermore, by-products such as the sodium salt of curcumin, weakly unstable acids such as $H_2CO_3$, $CO_2$, and water were generated, all of which being eliminated from the environment after rinsing with distilled water. The produced Cur-NPs did not contain any hazardous, toxic, and mutagenic chemicals such as dichloromethane, ethyl acetate, and Tween 80, which are commonly used when producing Cur-NPs. In most studies, dimethyl sulfoxide (DMSO) has been used as the primary solvent for curcumin powder [29]. Due to its dermal complications, irritation, and allergy, this solvent was not utilized in this research. In this study, ethanol was used as primary solvent which evaporates at high temperatures and water-soluble Cur-NPs was added to Chi-Ag NC solution. In another work, 1 M NaOH was used as the main solvent, and the curcumin oxide solution was utilized to produce silver curcumin NC [11]. Khan et al. (2019) presented a rapid procedure for curcumin silver nanoparticles synthesis at a pH of 9.92 in an alkaline medium. In their research, curcumin was used as a reducing and a capping agent in combination with silver nitrate as the silver precursor [30].

### Characterization of Cur-NPs

The particle size and distribution of Cur-NPs were evaluated by SEM, and DLS analysis. Under SEM, the Cur-NPs appeared as clusters of round particles at approximately 100 nm in dimension. Likewise, the DLS results displayed an average size of 97.7 nm for the Cur-NPs with polydispersity index (PDI) of 0.0913, indicating an excellent uniformity of these NPs. The PDI is a metric of particle uniformity; the lower the value, the more uniform the particles are.(Fig. 1). In the study of Bhavana et al. (2011), however, Cur-NPs with mediocre sizes of about 50 nm were obtained [31]. The absorption spectra of Cur-NPs is shown in Fig. 2. The absorption bands of Cur-NPs at 420 nm pertain to the presence of the aromatic ring in their structure [32].

### Characterization of NCs

UV–VIS spectrophotometry of Chi-Ag NC had a peak at 400 nm (Fig. 2). This peak does not occur when chitosan is measured separately. According to Anandalakshmi et al. (2016), this band relates to the absorption of Ag-NPs within the extend of 400–450 nm owing to the stimulation of surface plasmon vibration [33].

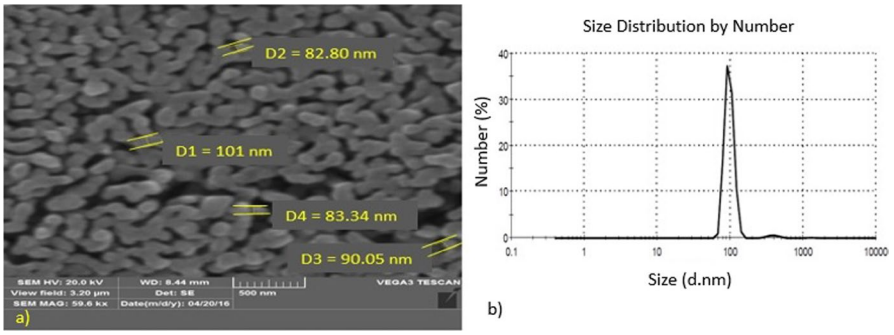


**Fig. 1** Size characterization of Cur-NPs: **a** SEM image, and **b** DLS analysis

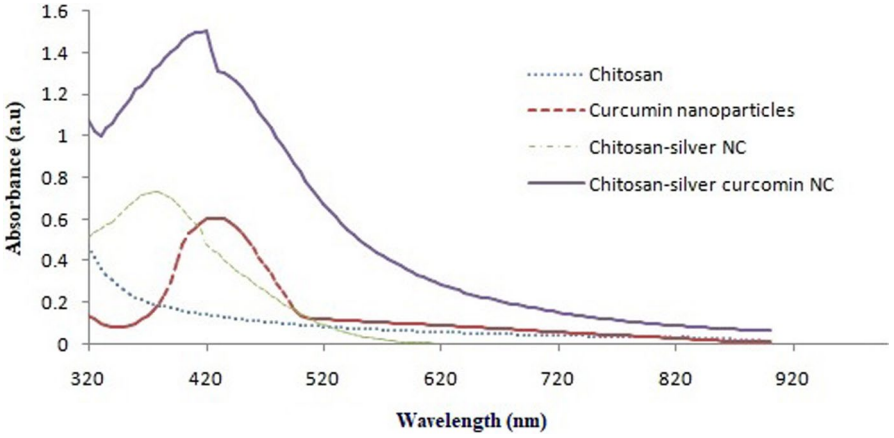


**Fig. 2** Comparative UV–visible spectra of Chitosan (…), Cur-NPs (--), Chi-Ag NC (-.-.) and Chi-Ag-Cur NC (-)

The Chi-Ag-Cur NC spectrum showed the highest absorptions at 400 and 420 nm (Fig. 2). The absorption band of curcumin appeared at 420 nm which is in agreement with the results of [34]. Curcumin is known to have a long and intense wavelength absorption in the visible range from 420–580 nm [32].

DLS findings revealed that 99.9% of Ag-NPs in Chi-Ag NC have a size of 30 nm with PDI of 0.09. The average size reported by DLS agrees with the SEM imaging, which reveals that the diameters of the NPs are between 10 and 30 nm. (Fig. 3). On the surface of Chi-Ag NC film in SEM images, Ag-NPs were seen as white particles around 20 nm in dimension which have accumulated at some places (Fig. 3). 26 synthesized Ag-NPs spherical aggregates wrapped by chitosan with sizes ranging from 6 to 18 nm [26], which is consistent with our findings. Nate et al. (2018) did, however, obtain Chi-Ag NPs with dimension ranging from 2 to 6 nm [35].

DLS results of Chi-Ag-Cur NC showed that 91.6% of NC have a size of 104 nm with PDI of 0.0897 which is consistent with the SEM image (Fig. 4). Because of

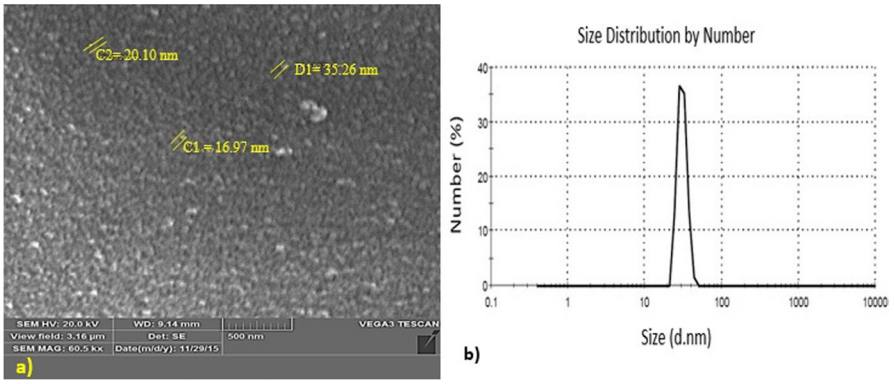


**Fig. 3** Size characterization of Chi-Ag NC: **a** SEM image, and **b** DLS analysis

the presence of ions near the NPs, larger sizes are expected in DLS compared to SEM. On the Chi-Ag-Cur NC surface, spherical to oval Cur-NPs with diameters smaller than 110 nm were detected along with Ag-NPs (Fig. 4). However, Ma et al. (2020) reported the average diameter of curcumin-loaded chitosan NPs to be $134.37 \pm 1.99$ nm [36].

EDX spectroscopy was used to determine the elemental composition of the produced NCs. Chitosan contains carbon, nitrogen, and oxygen which is confirmed by the presence of the C, O, and N peaks in the EDX spectra. In the same manner, Ag ions indicate the presence of Ag-NPs in the composite (Fig. 5). Carbon and oxygen rising percentages in Chi-Ag-Cur NC indicate the presence of curcumin, an organic compound that contains these elements (Fig. 5).

The FTIR spectra of (a) chitosan and (b) Chi-Ag NC are displayed in Fig. 6. The FT-IR spectrum of chitosan demonstrate amide A and amide B bands at wavenumbers of 3445 and 2920 $cm^{-1}$. The amide A emerges chiefly because of O–H and

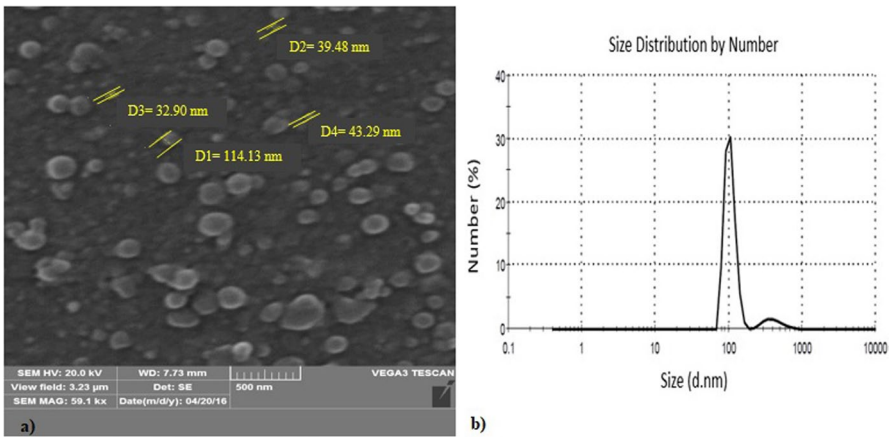


**Fig. 4** Size characterization of Chi-Ag-Cur NC: **a** SEM image, and **b** DLS analysis

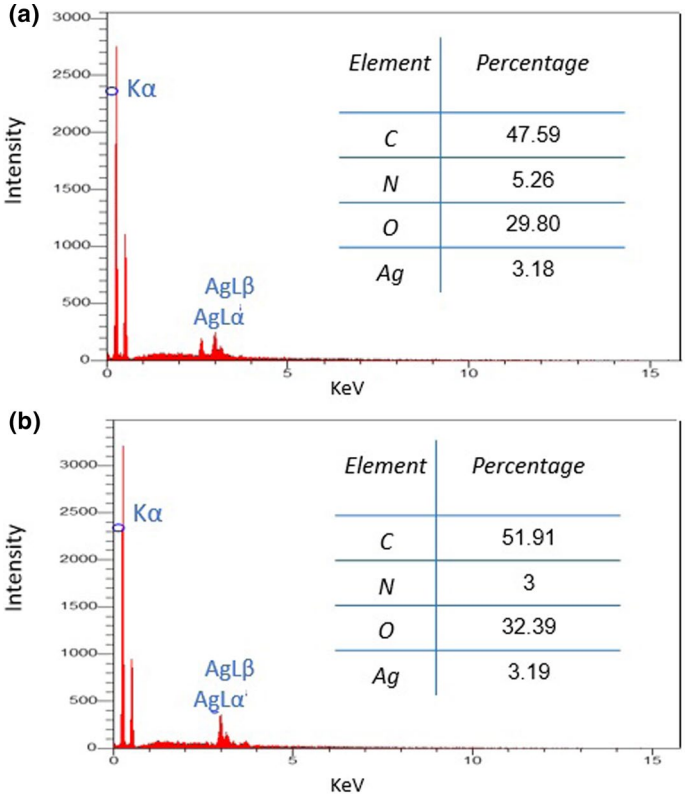


**Fig. 5** EDX plot of **a** Chi-Ag NC, **b** Chi-Ag-Cur NC

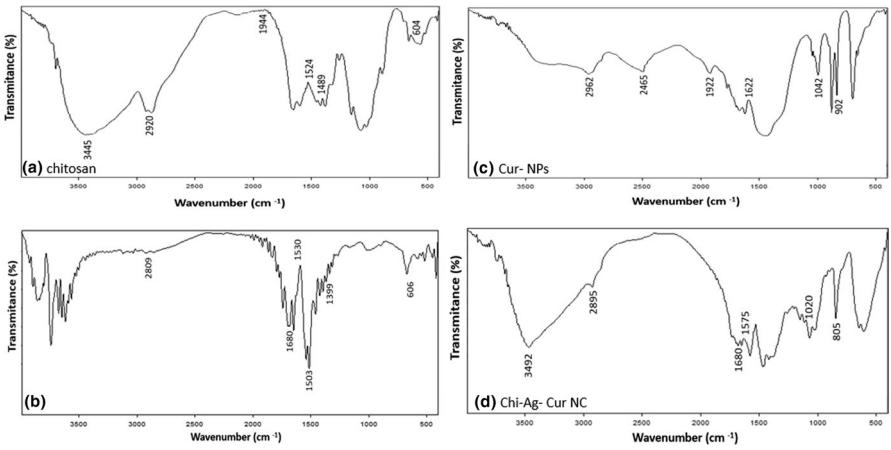


**Fig. 6** FTIR spectra of **a** Chitosan, **b** Chi-Ag NC, **c** Cur-NPs, and **d** Chi-Ag-Cur NC

N–H extending vibrations. The amide B arises chiefly due to the extending vibrations of the aliphatic –CH bonds [37, 38]. The FT-IR spectrum of Chi-Ag NC indicated some alterations compared to chitosan. A new peak was appeared at wavenumber of 2809 $cm^{-1}$ which related to amide B. Interactions between amine and amide groups in the structure of chitosan and Ag-NPs can cause these changes. In addition, the three amide bands of I, II, and III of Chi-Ag NC shifted to 1680 $cm^{-1}$, 1530 $cm^{-1}$, and 1399 $cm^{-1}$, which indicates the chelating of Ag-NPs with chitosan amino and hydroxyl groups. Figure 6 shows the FTIR spectra of (c) Cur-NPs, and (b) Chi-Ag-Cur NC. Absorption peaks between 1450 and 1622 $cm^{-1}$ correspond to aromatic and phenolic bands. Other peaks between 1000 and 1300 $cm^{-1}$ are related to symmetric and asymmetric C–O–C groups [11]. These peaks were detected in the spectrum of both Cur-NPs and Chi-Ag- Cur NCs. The formation of hydrogen bonds between curcumin with silver nanoparticles or chitosan chains in the Chi-Ag-Cur NC structure can be interpreted as this. The same results have been reported in the previous studies on curcumin loading in chitosan NPs [39].

The XRD pattern was measured to identify the crystalline structure of Cur-NPs and their changes after the addition to Chi-Ag NC. The XRD pattern of Chi-Ag NC shows a sharp peak at $2\theta = 16.96°$, which corresponds to the characteristic peak for chitosan chains [27], thus showing its high degree of crystallinity. The XRD pattern of Cur-NPs exhibited the characteristic peaks at $2\theta$ values of 32.35°, 33.93°, 37.96°, and 45.3°. Characteristic peaks of Cur-NPs were observed in the XRD pattern of Chi-Ag-Cur NC, showing that the NC is composed of Cur-NPs. Also, the shift in characteristic peak of chitosan to 11.39° in the XRD pattern of Chi-Ag-Cur NC is shown in Fig. 7.

## Antibacterial activity

Chi-Ag NC, Chi-Ag-Cur NC, and Cur-NPs were examined for antibacterial activity against clinical bacterial isolates related with wound infections, as well as some standard bacterial strains. The results obtained are set out in Fig. 8 and Table 1. The results revealed that Chi-Ag-Cur NC has a better antibacterial activity. As shown in Table 1, Cur-NPs have higher MIC and adding Cur-NPs to Chi-Ag NC leads to lower MIC of Chi-Ag-Cur NC. Furthermore, both synthesized NC were more effective against standard isolates rather than clinical isolates. Clinical strains are likely to have genetic and structural changes due to their high antibiotic resistance.

This hypothesis that Chi-Ag NC has the better antibacterial effect compared to pure chitosan or Ag-NPs, has been confirmed in many studies [26, 35, 40–42]. For example, [41] demonstrated the superior antibacterial property of Chi-Ag-NPs compared with pure chitosan or AgNPs against Methicillin-Resistant Strains of *Staphylococcus aureus*, with a MIC of 1.2 µg/mL [41]. Chi-Ag NC was reported by [7] to have a strong antimicrobial effect against all tested microorganisms at MICs of 1.69 µg/mL (*E. coli*) and 3.38 µg/mL (*K. pneumoniae*) [7]. 26 have also reported the antimicrobial activity of Chi-AgNPs against *P. aeruginosa*, providing 92% inhibition with a MIC of 50 µg/mL) [26]. Compared to previous studies, our results showed that the antibacterial property of Chi-Ag NC occurs at relatively lower MIC

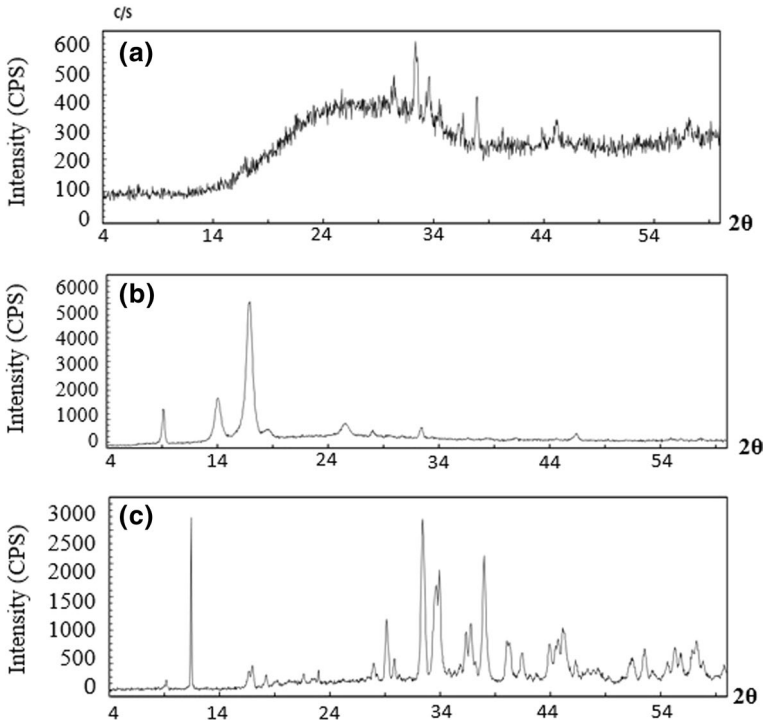


**Fig. 7** XRD pattern of **a** Cur-NPs, **b** Chi-Ag NC, and **c** Chi-Ag-Cur NC

values. The MIC of Chi-Ag NC was 5.85 µg/mL for clinical isolates and 0.73 µg/mL for standard strains. All studies regarding chitosan's bactericidal properties have shown that amino acids groups with positive charge in the chitosan structure interact with negative bacterial cell wall components; hence, interfering with their function and allowing proteins and other intracellular substances to discharge [9]. Chitosan stabilizes and prevents Ag-NP agglomeration in the Chi-Ag NC structure, causing their binding to the bacterial cell wall. Ag-NPs with positive charge bond to peptidoglycan thiol groups, causing bacterial cell lysis. Furthermore, microbial DNA is affected when respiratory enzyme pathways are blocked [42, 43].

Natural polymers such as chitosan have also been used for the preparation of curcumin loaded NPs. Curcumin nanoformulations aim to achieve increased solubilization of curcumin [44]. Trapping of curcumin in Chi-Ag- NC along with Ag-NPs to act as nano-reinforcements within the chitosan matrix leads to strengthening the antibacterial polymeric nano-system. In our research, Chi-Ag-Cur NC inhibited the growth of all tested microorganisms at relatively low MIC values. The MIC of Chi-Ag-Cur NC was 0.61 µg/mL for standard strains and 1.22 µg/mL for clinical isolates. The reduced size of curcumin in the form of nanoparticles is responsible for the more effective penetration to cells resulting in lower MICs. Cur-NPs' antibacterial function acts through a variety of mechanisms, including interference in cellular activities by targeting DNA and proteins, breakdown of their cell walls and

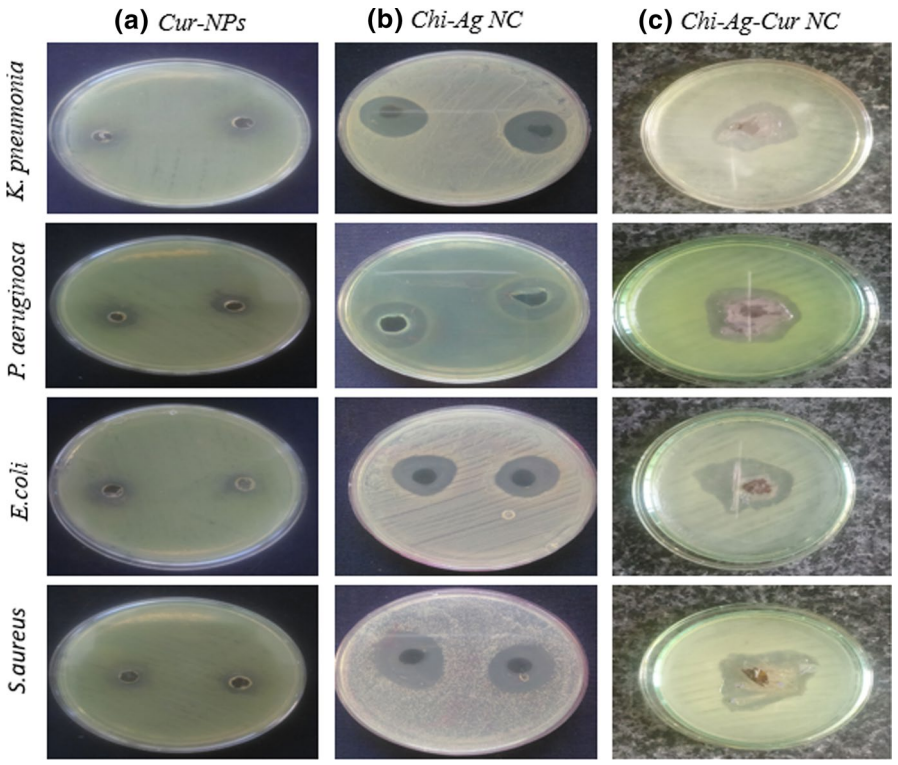


**Fig. 8** The antibacterial assay showing zone of inhibition effect of **a** Cur-NPs, **b** Chi-Ag NC, and **c** Chi-Ag-Cur NC

**Table 1** Antibacterial activities of Chi-Ag NC, Chi-Ag-Cur NC, and Cur-NPs against clinically and standard bacterial strains (MIC (μg/ml) results

| Bacterial strains | Cur-NPs MIC (μg/ml) | Chi-Ag NC MIC (μg/ml) | Chi-Ag-Cur NC MIC (μg/ml) |
|---|---|---|---|
| K5 | 46.87 | 5.85 | 1.22 |
| Ps14 | 46.87 | 5.85 | 1.22 |
| E18 | 23.43 | 5.85 | 1.22 |
| S3 | 23.43 | 2.92 | 1.22 |
| *S. aureus* 25923 | 2.92 | 0.73 | 0.61 |
| *K. pneumoniae* 7000603 | 5.85 | 0.73 | 0.61 |
| *P. aeruginosa* 27853 | 5.85 | 0.73 | 0.61 |
| *E. coli* 25922 | 5.85 | 0.73 | 0.61 |

preventing transit across their cell membrane, and inhibition of bacterial quorum sensing [17]. Therefore, these properties make Cur-NPs an interesting option for antibiotic-resistant strains.

Our finding has established that Chi-Ag NC and Chi-Ag-Cur NC are effective in eradicating bacterial biofilms (Table 2). MBIC90 of Chi-Ag-Cur NC were 19.53 and 4.88 µg/mL for clinical and standard strains, respectively. Chi-Ag-Cur NC has appeared better results in preventing the development and removing bacterial biofilms, suggesting that Chi-Ag-Cur NC displayed high biofilm hindrance at very low concentrations. Interestingly, Cur-NPs had a minor antibiofilm effect at 375 and 46.87 µg/mL for clinical and standard strains, respectively. These results suggest that the attachment of Cur-NPs to the chitosan surface is improving its biological activity which could upgrade the penetration of NPs into the deepest layers of the biofilm. NPs denote a hopeful platform for antibiofilm technologies due to their improved permeation into biofilms and capability of size, shape, and surface functionalization [45].

Nanocurcumin has the benefit of overcoming solubility challenges existing for curcumin in its normal shape. Shariati et al. (2019) proved how nanocurcumin could damage biofilm growth by downregulating numerous *P. aeruginosa* genes responsible for the coding of proteins correlated to efflux pumps, adhesion, and biofilm formation [46]. Other studies demonstrated that nanocurcumin also disturbs biofilm formation on a protein inhibition level [45]. Additionally, the application of polysaccharides such as chitosan, alginate, starch, and cellulose as nanocarrier polymers is particularly interesting given the high biocompatibility of these materials with the biofilm matrix [45]. The concentration of Chi-Ag-Cur NC needed for biofilm eradication is higher than the concentration of Chi-Ag-Cur NC that can inhibit biofilm which is thought to be related to the aggregation of NPs interacting with the biofilm matrix.

### Cytotoxicity test

Since Ag-NPs have exhibited toxicity to human cells [47, 48], cytotoxicity of the prepared NCs was studied on NHDF cells using the MTT assay. Results showed that cell survival rate was 85.98% at a concentration of 1000 µg/ml of Chi-Ag NC and 81.76%for Chi-Ag-Cur NC. No toxicity was observed at lower concentrations (Fig. 9). This is due to the fact that the stabilization of Ag-NPs in chitosan biopolymer impedes the internalization of Ag-NPs by eukaryotic cells. Similarly, [49] demonstrated antibacterial efficacy of polysaccharide coated Ag-NPs produced from chitosan on eukaryotic cells while causing no toxicity [49]. The cytotoxic concentration of the prepared NCs was found to be notably higher than the MIC. This result is further supported by the work of [50] in which Cur–Ag-NPs were shown to be toxic at higher concentrations compared with the bacterial MIC [50].

## Conclusions

In recent years, nanocomposites comprised of NPs have shown good bactericidal results. There has been a rise in research over the past few years on chitosan-based nanocomposites, particularly those containing NP reinforcements. The present work

**Table 2** Antibiofilm activities of Chi-Ag NC, Chi-Ag-Cur NC, and Cur-NPs against clinically and standard bacterial strains (MBIC 90 and MBEC90 (µg/ml) results)

| Bacterial strains | Chi-Ag NC | | Chi-Ag-Cur NC | | Cur-NPs | |
|---|---|---|---|---|---|---|
| | MBIC 90 (µg/ml) | MBEC 90 (µg/ml) | MBIC 90 (µg/ml) | MBEC 90 (µg/ml) | MBIC 90 (µg/ml) | MBEC 90 (µg/ml) |
| K5 | 23.43 | 93.75 | 19.53 | 39.06 | 375 | 750 |
| Ps14 | 46.87 | 93.75 | 19.53 | 39.06 | 375 | 750 |
| E18 | 46.87 | 93.75 | 19.53 | 39.06 | 187.5 | 750 |
| S3 | 23.43 | 93.75 | 19.53 | 39.06 | 375 | 750 |
| *S. aureus* 25923 | 11.71 | 23.43 | 4.88 | 19.53 | 46.87 | 93.75 |
| *K. pneumoniae* 7000603 | 11.71 | 23.43 | 4.88 | 19.53 | 46.87 | 93.75 |
| *P. aeruginosa* 27853 | 11.71 | 23.43 | 4.88 | 19.53 | 46.87 | 93.75 |
| *E. coli* 25922 | 11.71 | 23.43 | 4.88 | 19.53 | 46.87 | 93.75 |

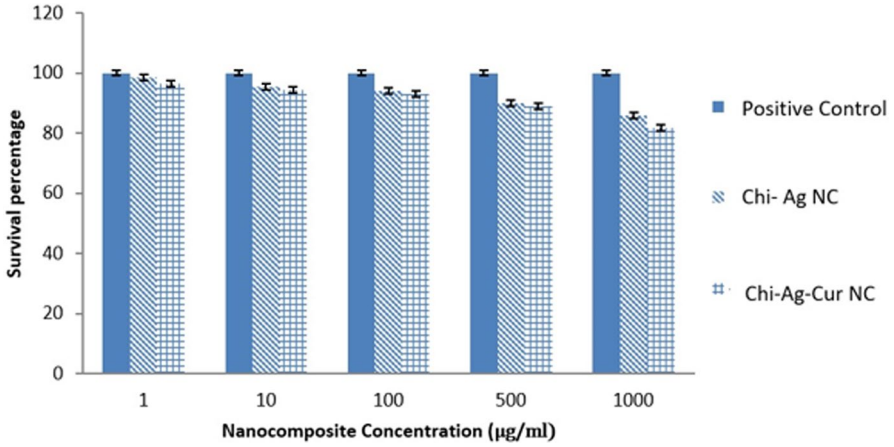


**Fig. 9** Comparison of cell survival after 24-h exposure to different concentrations of Chi-Ag NC and Chi-Ag-Cur NC using MTT assay

demonstrated a simple green synthesis method for producing Chi-Ag NC. Furthermore, we also developed a promising method in order to combine Chi-Ag NC with a natural compound (curcumin). In fact, Chi-Ag NC was reinforced with Cur-NPs. Two prepared NCs were characterized using UV–VIS spectrophotometry, FTIR, XRD, EDX, DLS, and SEM techniques. In addition, antibacterial tests showed that Chi-Ag-Cur NC has a higher antibacterial activity against both clinical and standard isolates. Also, Chi-Ag-Cur NC films can be used as antibiofilm surface coatings. This property may be highly valuable in preventing biofilm formation in burn wound infections.

**Acknowledgements** The authors would like to thank from the colleagues of Microbiology Laboratories of Alzahra University, Tehran, Iran.

**Author contribution** ZR: Investigation; Methodology, Resources. EMQ: Writing—original draft, Writing—review & editing. RKK: Project administration, Methodology, Supervision. FF: Methodology, Supervision, Resources.

## Declarations

**Conflict of interest** The authors declare they have no financial interests.

## References

1. Souto EB, Ribeiro AF, Ferreira MI, Teixeira MC, Shimojo AAM, Soriano JL (2020) New nanotechnologies for the treatment and repair of skin burns infections. Int J Mol Sci 21:393
2. Friedman ND, Temkin E, Carmeli Y (2016) The negative impact of antibiotic resistance. Clin Microbiol Infect 22:416–422
3. Sharmin S, Rahaman M, Sarkar C, Atolani O, Islam MT, Adeyemi OS (2021) Nanoparticles as antimicrobial and antiviral agents: a literature-based perspective study. Heliyon 7:e06456

4. Rayara A, Babaladimath G, Ambalgi A, Chapi S (2020) An eco-friendly synthesis, characterization and antibacterial applications of gellan gum based silver nanocomposite hydrogel. Mater Today: Proc 23:211–220
5. Sharanappa C, Ambalgi AP, Babaladimath G (2019) Gellan gum based silver nanocomposite hydrogel: preparation, characterisation and anti-bacterial study. Mater Today: Proc 18:3937–3945
6. Kumar SSD, Rajendran NK, Houreld NN, Abrahamse H (2018) Recent advances on silver NP and biopolymer-based biomaterials for wound healing applications. Int J Biol Macromol 115:165–175
7. Lima DDS, Gullon B, Cardelle-Cobas A et al (2017) Chitosan-based silver nanoparticles: a study of the antibacterial, antileishmanial and cytotoxic effects. J Bioact Compat Polym 32:397
8. Shao J, Yu N, Kolwijck E, Wang B, Tan KW, Jansen JA, Walboomers XF, Yang F (2017) Biological evaluation of silver nanoparticles incorporated into chitosan-based membranes. Nanomed J 12:2771
9. Shah A, Yameen MA, Fatima N, Murtaza G (2019) Chemical synthesis of chitosan/silver nanocomposites films loaded with moxifloxacin: their characterization and potential antibacterial activity. Int J Pharm 561:19–34
10. Othman N, Masarudin MJ, Kuen CY, Dasuan NA, Abdullah LC, Jamil SNAM (2018) Synthesis and optimization of chitosan nanoparticles loaded with l-ascorbic acid and thymoquinone. Nanomaterials 8:920
11. Abd El-Hady MM, El-Sayed Saeed S (2020) Antibacterial properties and pH sensitive swelling of insitu formed silver-curcumin nanocomposite based chitosan hydrogel. Polymers 12:1–14
12. Niu X, Wei Y, Liu Q, Yang B, Ma N, Li Z, Zhao L, Chen W, Huang D (2020) Silver-loaded microspheres reinforced chitosan scaffolds for skin tissue engineering. Eur Polym J 134:109861
13. Dankane I, Chapi S, Bello K (2020) The potential of silver nanoparticles as heterogeneous catalysts for generation of biodiesel from vegetable oils. AIP Conf Proc 2244(1):110017
14. Kalaivani R, Maruthupandy M, Muneeswaran T, Hameedha Beevi A, Anand M, Ramakritinan CM, Kumaraguru AK (2018) Synthesis of chitosan mediated silver nanoparticles (Ag NPs) for potential antimicrobial applications. Front Lab Med 2:30–35
15. Alven S, Nqoro X, Aderibigbe B (2020) Polymer-based materials loaded with curcumin for wound healing application. Polymers 12:2286
16. Okur ME, Karantas ID, Şenyiğit Z, Okur NÜ, Siafaka PI (2020) Recent trends on wound management; new therapeutic choices based on polymeric carriers. Asian J Pharm Sci 15:661–684
17. Trigo-Gutierrez JK, Vega-Chacón Y, Soares AB, Mima EGDO (2021) Antimicrobial activity of curcumin in nanoformulations: a comprehensive review. Int J Mol Sci 22:7130
18. Rajabloo Z, Farzaneh F, Kermanshahi RK (2016) Synthesis of chitosan-silver nanocomposite films through green method. Int J Innov Res Sci Eng Technol 5:11696–11699
19. Zheng Z, Zhan XD, Carbo C, Clark CA, Nathan Y (2010) Sonication assisted synthesis of polyelectrolyte coated curcumin nanoparticles. Langmuir 26:7679–7781
20. CLSI (2012) Methods for dilution antimicrobial susceptibility tests for bacteria that grow aerobically, Approved Standard, 9th ed., CLSI document M07-A9. clinical and laboratory standards institute, 950 West Valley Road, Suite 2500, Wayne, Pennsylvania p. 19087, USA
21. Stepanovic S, Vukovic D, Hola V, Di Bonaventura G, Djukic S, Cirkovic I, Ruzicka F (2007) Quantification of biofilm in microtiter plates: overview of testing conditions and practical recommendations for assessment of biofilm production by staphylococci. Acta Pathol Microbiol Scand 115:891–899
22. Kheiri F, Kermanshahi RK, Feizabadi MM (2020) The inhibitory effects of lactobacillus supernatants and their metabolites on the growth and biofilm formation of *Klebsiella pneumonia*. Infect Disord Drug Targets 20:902–912
23. Freire PLL, Albuquerque AJR, Farias IAP et al (2016) Antimicrobial and cytotoxicity evaluation of colloidal chitosan–silver nanoparticles–fluoride nanocomposites. Int J Biol Macromol 93:896–903
24. Abdellah AM, Sliem MA, Bakr M, Amin RM (2018) Green synthesis and biological activity of silver-curcumin nanoconjugates. Future Med Chem 10:2577–2588
25. Cao XL, Cheng C, Ma YL, Zhao CS (2010) Preparation of silver nanoparticles with antimicrobial activities and the researches of their biocompatibilities. J Mater Sci: Mater Med 21:2861
26. Rajivgandhi G, Maruthupandy M, Veeramani T, Quero F, Li WJ (2019) Anti-ESBL investigation of chitosan/silver nanocomposites against carbapenem resistant *Pseudomonas aeruginos*. Int J Biol Macromol 132:1221
27. Thomas V, Yallapu MM, Sreedhar B (2009) Fabrication, characterization of chitosan/nanosilver film and its potential antibacterial application. J Biomater Sci 20:2129–2144

28. Vimala K, Yallapu MM, Varaprasad K, Reddy NN, Ravindra S, Naidu NS (2011) Fabrication of curcumin encapsulated chitosan-PVA silver nanocomposite films for improved antimicrobial activity. J biomater nanobiotechnol 02:55–64
29. Krausz AE, Adler BL, Cabral V et al (2015) Curcumin-encapsulated NPs as innovative antimicrobial and wound healing agent. Nanomedicine 11:195–206
30. Khan MJ, Shameli K, Sazili AQ, Selamat J, Kumari S (2019) Rapid green synthesis and characterization of silver nanoparticles arbitrated by curcumin in an alkaline medium. Molecules 24:719
31. Bhawana B, Basniwal RK, Buttar HS, Jain VK, Jain N (2011) Curcumin nanoparticles: preparation, characterization, and antimicrobial study. J Agric Food Chem 59:2056–2061
32. Sofyan N, Situmorang FW, Ridhova A, Yuwono AH, Udhiarto A (2018) Visible light absorption and photosensitizing characteristics of natural yellow 3 extracted from Curcuma Longa L. for DyeSensitized solar cell. OP Conf Ser Earth Environ Sci 105:012073
33. Anandalakshmi K, Venugobal J, Ramasamy V (2016) Characterization of silver nanoparticles by green synthesis method using Pedalium murex leaf extract and their antibacterial activity. Appl Nanosci 6:399–408
34. Sharma K, Agrawal SS, Gupta M (2012) Development and validation of UV spectrophotometric method for the estimation of curcumin in bulk drug and pharmaceutical dosage forms. Int J Drug Dev Res 4:375–380
35. Nate Z, Moloto MJ, Mubiayi PK, Sibiya PN (2018) Green synthesis of chitosan capped silver nanoparticles and their antimicrobial activity. MRS Adv 3:2505
36. Ma S, Moser D, Han F, Leonhard M, Schneider-Stickler B, Tan Y (2020) Preparation and antibiofilm studies of curcumin loaded chitosan nanoparticles against polymicrobial biofilms of *Candida albicans* and *Staphylococcus aureus*. Carbohydr Polym 241:116254
37. Venkatesham M, Ayodhya D, Madhusudhan A, Veera Babu N, Veerabhadram G (2014) A novel green one-step synthesis of silver nanoparticles using chitosan: catalytic activity and antimicrobial studies. Appl Nanosci 4:113
38. Senthilkumar P, Yaswant G, Kavitha S, Chandramohan E, Kowsalya G, Vijay R, Sudhagar B, Kumar DSRS (2019) Preparation and characterization of hybrid chitosan-silver nanoparticles (Chi-Ag NPs); a potential antibacterial agent. Int J Biol Macromol 141:290
39. Jahromi MAM, Al-Musawi S, Pirestani M, Ramandi MF, Kazem Ahmadi K, Rajayi H, Hassan ZM, Kamali M, Mirnejad R (2014) Curcumin-loaded chitosan tripolyphosphate nanoparticles as a safe, natural and effective antibiotic inhibits the infection of *Staphylococcus aureus* and *Pseudomonas aeruginosa* in vivo. Iran J Biotechnol 12:e1012
40. Bardajee GR, Hooshyar Z, Rezanezhad H (2012) A novel and green biomaterial based silver nanocomposite hydrogel: synthesis, characterization and antibacterial effect. J Inorg Biochem 117:367–373
41. Holubnycha V, Kalinkevich O, Ivashchenko O, Pogorielov M (2018) Antibacterial activity of in situ prepared chitosan/silver nanoparticles solution against methicillin-resistant strains of *Staphylococcus aureus*. Nanoscale Res Lett 13:71
42. Polinarski MA, Beal ALB, Silva FEB, BernardiWenzel J, Burin GRM, Muniz GIB, Alves HJ (2021) New perspectives of using chitosan, silver, and chitosan– silver nanoparticles against multidrug-resistant bacteria. Part Part Syst Charact 38:2100009
43. Adeli M, Hosainzadegan H, Pakzad I, Zabihi F, Alizadeh M, Karimi F (2013) Preparing starchy foods containing silver NPs and evaluating antimicrobial activitiy. Jundishapur J Microbiol 6:1–7
44. Naksuriya O, Okonogi S, Schiffelers RM, Hennink WE (2014) Curcumin nanoformulations: a review of pharmaceutical properties and preclinical studies and clinical data related to cancer treatment. Biomaterials 35:3365–3383
45. Barros CHN, Casey E (2020) A review of nanomaterials and technologies for enhancing the antibiofilm activity of natural products and phytochemicals. ACS Appl Nano Mater 3:8537–8556
46. Shariati A, Asadian E, Fallah F, Azimi T, Hashemi A, Sharahi JY, Moghadam MT (2019) Evaluation of nano-curcumin effects on expression levels of virulence genes and biofilm production of multidrug-resistant *Pseudomonas aeruginosa* isolated from burn wound infection in Tehran. Iran Infect Drug Resist 12:2223–2235
47. Akter M, Sikder MT, Rahman MM, Ullah AKMA, Hossain KFB, Banik S, Hosokawa T, Saito T, Kurasaki MA (2018) A systematic review on silver nanoparticles-induced cytotoxicity: physicochemical properties and perspectives. J Adv Res 9:1–16
48. Avalos A, Haza AI, Mateo D, Morales P (2016) Interactions of manufactured silver nanoparticles of different sizes with normal human dermal fibroblasts. Int Wound J 13:101–109

49. Travan A, Pelillo C, Donati I, Marsich E, Benincasa M, Scarpa T, Semeraro S, Turco G, Gennaro R, Paoletti S (2009) Non-cytotoxic silver nanoparticle-polysaccharide nanocomposites with antimicrobial activity. Biomacromol 10:1429–1435
50. Jaiswal S, Mishra P (2018) Antimicrobial and antibiofilm activity of curcumin-silver NPs with improved stability and selective toxicity to bacteria over mammalian cells. Med Microbiol Immunol 207:39–53